5115/91
LIBRARY

IC/91/137
INTERNAL REPORT
(Limited Distribution)

International Atomic Energy Agency
and
United Nations Educational Scientific and Cultural Organization
INTERNATIONAL CENTRE FOR THEORETICAL PHYSICS

FORMATION MECHANISMS OF AMORPHOUS CLUSTERS IN Mn^+ IMPLANTED THIN Al FILMS

C.A. Majid *
International Centre for Theoretical Physics, Trieste, Italy.

ABSTRACT

The amorphization process of thin Al films by successive implantation with Mn^+ ions at RT and LNT was studied by X–ray diffraction and Rutherford backscattering. For each Mn concentration strain and crystallite size were determined from X–ray line broadening. For RT implantation amorphization sets in at approximately 1 at% Mn by thermally activated local atomic rearrangements which lead to the formation of amorphous clusters. At LNT, a supersaturated solid solution is formed at mean Mn concentrations below 5 at%. At higher Mn concentrations amorphous clusters are formed throughout the sample in regions where the local strain level has reached a threshold value which occurs at a critical local Mn concentration of 8.5 at%. The results indicate a preferential short–range migration of Mn atoms from the remaining crystalline material toward the amorphous formed at LNT causing a Mn depletion and partial recovery of the crystalline regions.

MIRAMARE – TRIESTE

June 1991

* Permanent address: Nuclear Materials Division, Pakistan Institute of Nuclear Science and Technology (Pinstech), P.O. Office Nilore, Islamabad, Pakistan.

REFERENCE

1. Introduction

Amorphous materials are subject to many experimental investigations since they exhibit a wide range of interesting properties. Recently, the amorphous phase and its formation mechanisms have been studied by various methods. Ion implantation experiments are particularly suitable for a study of the mechanisms since the amorphization process can be studied as a function of composition by successive ion implantations.

In previous papers [1,2] the formation mechanisms of the amorphous phase were studied in the ion-target system Mn→Al for different target temperatures. It was found that the strains induced by the forced introduction of Mn impurity atoms lead to severe distortions of the Al host lattice and thus provide the driving force for the c→a transformation. Amorphization occurs by the formation of small amorphous clusters of given, implantation temperature dependent composition.

In this paper further details of the amorphization process in Mn implanted Al thin films are reported. Strain and crystallite size parameters derived from X-ray line broadening data provide new information on the evolution of the defect structure during amorphization, in particular, a Mn depletion of the crystalline regions in favor of the formation of amorphous clusters was found at LNT implantation.

2. EXPERIMENTAL AND ANALYSIS

Polycrystalline Al films with thickness of approximately 250 nm were prepared by dc magnetron sputtering. The composition of the films was modified in steps by successive Mn^+ ion implantations and was checked by Rutherford backscattering (RBS). For details, see Refs. [1,2]. X-ray spectra of the thin film samples were measured after each implantation step using a two-circle diffractometer with Bragg-Brentano focusing geometry. The Cu rotating anode generator was operated at 8 kW. Pure $CuK\alpha_1$ radiation was obtained by using a

quartz monochromator. The instrumental resolution of the diffractometer was determined by measuring several reflections of a Ge single crystal. The integral breadth $\delta 2\Theta$ of these reflections increased linearly with scattering angle 2Θ from 0.092° at $2\Theta = 27°$ to 0.100° at $2\Theta = 88°$. X-ray spectra of the thin films were measured in the angular range of 34° to 90° in 2Θ, and the integral breadths of the five fcc Al reflections detected in that angular range were determined.

Strain and crystallite size analyses were performed based on a method described by Klug and Alexander [3]. This method uses integral line breadths as a measure of line broadening. In a first step the instrumental broadening is separated from the "physical" line broadening by applying the parabolic relationship [3,4]. Strain and size parameters are obtained by plotting $\gamma = (\delta 2\Theta)^2/\tan^2\Theta$ versus $x = \delta 2\Theta/(\tan\Theta\sin\Theta)$ for several reflections, where $\delta 2\Theta$ is the physical line breadth. The slope of the lines (least-squares fits through the data points) is inversely proportional to the crystallite size. The ordinate intercept is proportional to the square of the strain.

Representative examples of such plots are shown in Fig. 1 for a film implanted at LNT with different Mn concentrations. Note the different scales in Figs. 1a-d. Fig. 1a is a plot for an unimplanted sample. The different symbols stand for two different measurements and indicate the reproducibility of our results. The straight line fitted through the data points almost extrapolates to zero, revealing the low strain level in the as-deposited films. From the slope a crystallite size of 95 nm was calculated which is reasonable keeping in mind the film thickness of about 250 nm and the fact that the crystallite size is not the actual grain size but rather the size of coherently diffracting domains which may be separated by extended defects like dislocations, stacking faults, small-angle grain boundaries etc. [5]. Therefore, the crystallite size determined by this method may be taken as a measure of the density of extended defects, in particular, dislocations [6]. With increasing Mn concentration the slope of the

lines increases indicating a decrease of the crystallite size. The intercept, i.e. the strain also increases with Mn concentration.

For higher Mn concentrations (11.4 at% in Fig. 1d) only the crystallite size could be determined from the integral breadth of the (1 1 1) reflection, since the higher order reflections were severely attenuated. The value thus obtained for the crystallite size is still sufficiently accurate, since the strain contribution to the total line broadening is generally small compared to the size contribution especially at small scattering angles.

3. RESULTS AND DISCUSSION

Previous experiments [1,2] showed that for implantation at RT amorphization sets in at a Mn concentration near 1 at% by thermally activated local atomic rearrangements which lead to the formation of amorphous clusters. Further Mn implantation leads to a growth of the amorphous clusters by agglomeration and therfore to a linear increase of the amorphous fraction with Mn concentration [2].

For implantation at LNT the formation of amorphous clusters by local atomic rearrangements at small Mn concentration is not possible. Therefore, the Mn atoms are incorporated substitutionally, i.e. a supersaturated substitutional solution is formed at mean Mn concentrations below 5 at%. Due to the statistical distribution of Mn atoms there are regions of different local Mn concentrations. When the local Mn concentration in such a region has reached 8.5 at% the local strain level has reached a threshold value leading to amorphization of that region. The minimum size of the thus formed amorphous clusters was calculated to be 2×10^{-21} cm^{-3} from a fit of a statistical model [1,7,8] to the experimentally determined amorphization curve, which is a plot of the amorphous fraction versus Mn concentration [1].

In the following sections the variation of strain and crystallite size with Mn concentration will be reported for implantations at RT and LNT. The results will

be discussed with respect to the amorphization process. In particular, it will be shown that for implantation at LNT there are indications of a preferential short-range migration of Mn atoms from the remaining crystalline regions toward the amorphous clusters leading to a Mn depletion and partial recovery of the crystalline regions.

A. RT IMPLANTS

The impact of the Mn implantation on the crystallite size is shown in Fig. 2 which is a plot of the crystallite size versus Mn concentration. The crystallite size of the as-deposited films ranges from 80 to 100 nm. The implantation leads to a monotonic decrease of the crystallite size with Mn concentration. This is due to two different mechanisms: Firstly, the implantation of heavy ions into Al gives rise to the formation of a large number of dislocations. This was observed for Ni implantation into Al by channeling and TEM [9] and also for Mn implantation into Al [1]. In this way originally large crystallites are split up into incoherently diffracting domains and the crystallite size as determined by X-ray diffraction decreases. Secondly, starting at 1 at% Mn amorphous clusters of composition $Al_{0.82}Mn_{0.18}$ are formed [2]. This causes a shrinking of the crystallites simply because the amorphous clusters grow at the expense of the crystalline material as the Mn concentration is increased. At high Mn concentrations, where the samples are already mostly amorphous the crystallite size saturates at approximately 25 nm.

The strains in the films could be determined from the broadening of the X-ray lines at Mn concentrations of up to 10 at%. Beyond 10 at% Mn the line broadening is dominated by the effect of small crystallite size. Fig. 3 shows that the as-deposited films are only slightly strained. With increasing Mn concentration an accumulation of strain is observed reaching a maximum near 4 at% Mn. Strain determination by line broadening is sensitive to local strains around defects [5,10]. The strain accumulation is therefore attributed to

distortions associated with the high density of ion implantation induced extended defects and the formation of severely distorted regions in the vicinity of the implanted Mn atoms. The decrease of the strains at higher Mn concentrations is due to progressive amorphization and related partial recovery of the distorted crystalline material, in agreement with previous results [1,2].

B. LNT IMPLANTS

The effect of Mn implantation at LNT on the crystallite size of the Al thin film samples is shown in Fig. 4 which is a plot of the crystallite size versus Mn concentration. The crystallite size of the as deposited films is again in the range from 80 to 100 nm. Between 0 and 4 at% Mn the crystallite size decreases with Mn concentration. Unlike at RT, where the decrease in this concentration range was attributed to both the creation of a large number of extended defects and partial amorphization of the samples, implantation at LNT does not lead to amorphization below 4-5 at% Mn. This is shown in Fig. 5 which is a plot of the amorphous fraction versus Mn concentration. Therefore, the only mechanism leading to a decrease in the crystallite size in this concentration range is the creation of a large number of extended defects induced by the implantation of Mn ions.

Between 4 and 5 at% Mn a sudden increase of the crystallite size from 40 to 65 nm is observed. Ths increase coincides with the onset of amorphization as shown in Fig. 5, i.e. with the first formation of an appreciable number of amorphous clusters. Therefore, we conclude that this increase is due to a reduction of the density of extended defects in the damaged crystalline material induced by the onset of amorphization. A similar effect can be deduced from line broadening data published by Ewing et al. [11] who have studied the c→a transition in α-particle damaged natural $ZrSiO_4$.

This interpretation is further supported by X-ray line intensity and channeling data published previously [1], which indicate that the number of Mn atoms on

substitutional sites in the crystalline material is reduced by the onset of amorphization: As outlined in Ref. 1 the slope m in the modified Wilson plots, which are plots of the logarithmic ratio of integrated X-ray line intensities before and after implantation versus the square of the scattering vector, is a measure of the local distortions around the Mn atoms in the crystalline material. This quantity is plotted versus Mn concentration in Fig. 6. The linear increase of m with Mn concentration between 0 and 4-5 at% Mn is due to the increasing number density of Mn atoms which distort their local atomic environments severely. Once amorphization has set in these local distortions are relaxed within a concentration range of 2-3 at%. This effect can be explained by a reduction of the number density of Mn atoms in the crystalline material coinciding with the onset of amorphization. If the number density of Mn atoms in the crystalline material was left unchanged, we would expect a saturation of the local distortion in clear contrast to m-values shown in Fig. 6.

A further indication of this reduction is given by channeling data from which the fraction f_s of Mn atoms on substitutional lattice sites was determined. The substitutional fraction f_s, which is plotted versus Mn concentration in Fig. 7, is almost unity below 5 at%, i.e. prior to the onset of amorphization. Coinciding with the onset of amorphiaztion the substitutioanl fraction starts to decrease reaching zero at ≈12 at% Mn. However, if the remaining crystalline material was not affected by the newly formed amorphous clusters at Mn concentrations above 5 at% a constant, high substitutionality of the Mn atoms would be expected.

From the results presented above we draw the conclusion that the formation of amorphous clusters leads to a Mn depletion of the remaining crystalline material and to a decrease of the density of extended defects, in particular, dislocations. These effects are best understood by assuming that the amorphous clusters attract Mn atoms from adjacent crystalline regions, i.e. there is a preferential short-range migration of Mn atoms from crystalline regions toward

the newly formed amorphous clusters. The simultaneous decrease of the density of extended defects could be due to a pinning of dislocations by the impurity atoms: once the Mn impurity atoms are removed from the crystalline material the dislocations are annealed, possibly by annihilation at the interfaces with the amorphous clusters.

At Mn concentrations beyond 5 at% the growth of the amorphous phase that progressively consumes the crystalline regions becomes dominant, which accounts for the resumed reduction of the crystallite size as the amorphization proceeds. At high Mn concentrations, where the samples are already mostly amorphous, the crystallite size saturates at approximately 15 nm in a similar fashion as observed for the RT implants. The fact that the saturation value of the crystallite size at RT (25 nm) is larger than at LNT (15 nm) indicates that the remaining crystalline regions at high Mn concentrations are less damaged at RT than at LNT. This is due to a better annealing of the damage and a strong enhancement of the short-range migration of Mn atoms toward the amorphous clusters at higher temperatures.

The strains in the thin films implanted at LNT were determined at Mn concentrations below 7 at%. At higher Mn concentrations the considerable reduction of line intesities by partial amorphization and the domination of the line broadening by the size effect made an accurate determination of the strains difficult. Referring to Fig. 8, we observe an accumulation of strains at Mn concentrations below ≈5 at% in a similar fashion as observed at RT. This strain accumulation is therefore thought to be due to the same mechanisms: distortions around extended defects and severely distorted regions in the immediate vicinity of the Mn atoms. At a Mn concentration of 6.5 at%, i.e. after the onset of amorphization there is an indication for a strain relaxation but this effect could not be measured at higher Mn concentrations for intensity reasons.

4. SUMMARY AND CONCLUSIONS

The amorphization process in the ion-target system Mn→Al has been studied by Mn implantation into thin Al films held at RT and LNT. In both cases, amorphization occurs by formation of amorphous clusters. The formation mechanisms of the clusters depend strongly on target temperature:

At RT, vacancies and impurity atoms are mobile, so amorphous clusters are formed at low Mn concentrations by local atomic rearrangements leaving the remaining crystalline material essentially devoid of Mn atoms. Further Mn implantation leads to a growth of the amorphous clusters by agglomeration.

At LNT, there is essentially no atomic mobility, therefore the Mn atoms occupy mostly substitutional lattice sites at low concentrations. Only when locally a critical Mn concentration is reached such that the local strain value cannot be tolerated by the crystalline phase anymore, an amorphous cluster is formed. Once these amorphous clusters are formed the damage in the remaining crystalline regions is reduced by a preferential short-range migration of Mn atoms from these regions to the amorphous clusters, i.e. a Mn depletion of the crystalline material. Obviously, the presence of amorphous clusters is a prerequisite for this short-range Mn migration. The simultaneous reduction of the dislocation density in the crystalline regions may be due to a pinning of the dislocations by the Mn atoms and their subsequent annealing induced by the Mn depletion of the crystalline material.

A comparative study of the amorphization process by Ni implantation into Al is presently being carried out to test the applicability of the results and conclusions reported herein to other systems.

ACKNOWLEDGMENTS

The author acknowledges stimulating discussions with Professor Dr. W. Buckel. He would also like to thank Professor Abdus Salam, the International Atomic Energy Agency and UNESCO for hospitality at the International Centre for Theoretical Physics, Trieste and the Swedisch Agency for Research Cooperation with Developing Countries (SAREC), for financial support during his visist at the ICTP under the Associateship scheme.

REFERENCES

[1] A. Seidel, S. Massing, B. Strehlau, G. Linker, Phys. Rev. B 38, 2273 (1988)

[2] A. Seidel, S. Massing, B. Strehlau, G. Linker, Z. Phys. B (accepted for publication)

[3] H.P. Klug, L.E. Alexander, "X-Ray Diffraction Procedures for Polycrystalline and Amorphous Materials", (Wiley, New York, 1974), chapter 9

[4] C.N.J. Wagner and E.N. Aqua, "Advances in X-Ray Analysis", Vol. 7, (Plenum, New York, 1964), p. 46

[5] M.A. Krivoglaz, "Theory of X-Ray and Thermal Neutron Scattering by Real Crystals", (Plenum, New York, 1969), chapter IV

[6] L.H. Schwartz, J.B. Cohen, "Diffraction from Materials", 2nd edition, (Springer, Berlin, 1987), p. 391

[7] A. Benyagoub, Ph.D. Dissertation, Université de Paris-Sud, 1986 (unpublished)

[8] C. Cohen, A. Benyagoub, H. Bernas, J. Chaumont, L. Thome, M. Berti, A.V. Drigo, Phys. Rev. B 31, 5 (1985)

[9] S.T. Picraux, D.M. Follstaedt, P. Baeri, S.U. Campisano, G. Foti, E. Rimini, Rad. Effects 49, 75 (1980)

[10] E. Born, G. Paul, "Röntgenbeugung am Realkristall", (Thiemig, München, 1979)

[11] R.C. Ewing, B.C. Chakoumakos, G.R. Lumpkin, T. Murakami, MRS Bulletin, Vol. XII, No. 4, 58 (1987)

FIGURE CAPTIONS

Figure 1: X-ray line broadening data of a thin Al film implanted with different Mn concentrations. $y = (\delta 2\Theta)^2/\tan^2\Theta$ is plotted versus $x = \delta 2\Theta/(\tan\Theta\sin\Theta)$; $\delta 2\Theta$: integral breadth of an X-ray line at Θ. In this plot the slope of the fitted line is inversely proportional to the crystallite size and its intercept is proportional to the square of the strain [3].

Figure 2: Crystallite size of thin Al films implanted with Mn^+ ions at RT plotted versus Mn concentration. Different symbols stand for different samples.

Figure 3: Strain in thin Al films implanted with Mn^+ ions at RT plotted versus Mn concentration. Different symbols stand for different samples.

Figure 4: Crystallite size of thin Al films implanted with Mn^+ ions at LNT plotted versus Mn concentration. Different symbols stand for different samples.

Figure 5: Amorphous fraction of thin Al films implanted with Mn^+ ions at LNT plotted versus Mn concentration.

Figure 6: Slope m in the modified Wilson plots of thin Al films implanted with Mn^+ ions at LNT plotted versus Mn concentration as a measure of the local distortions around the Mn atoms. Different symbols stand for different samples.

Figure 7: Fraction of Mn atoms occupying substitutional lattice sites in an [110]-oriented Al single crystal implanted with Mn^+ ions at LNT plotted versus Mn concentration.

Figure 8: Strain in thin Al films implanted with Mn^+ ions at LNT plotted versus Mn concentration. Different symbols stand for different samples.

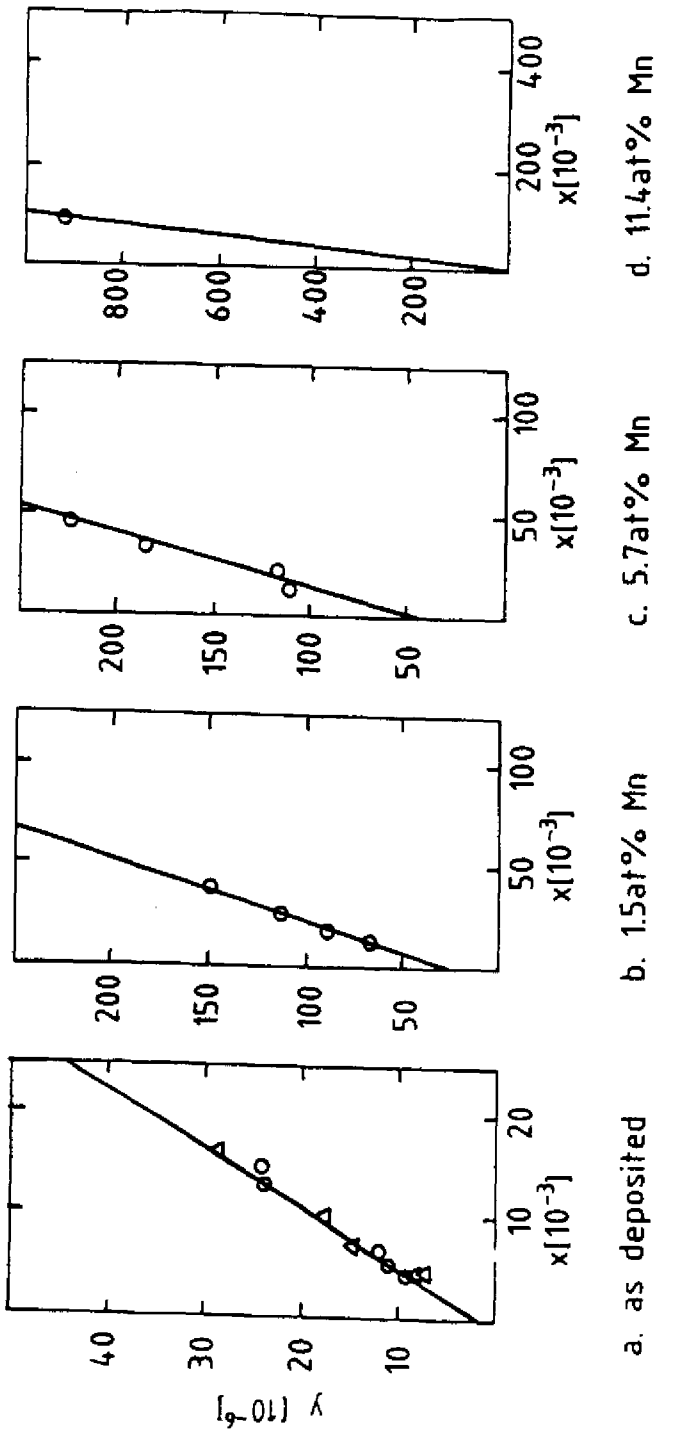

Fig.1

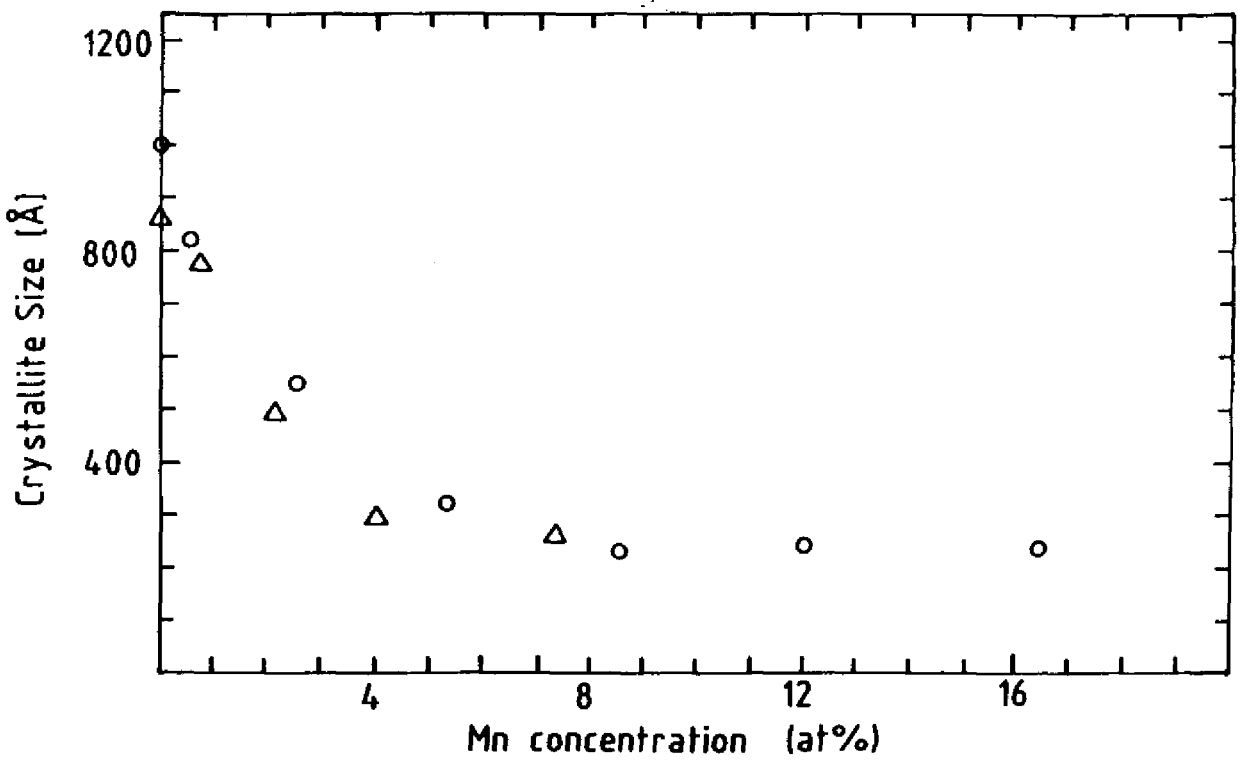
1200
800
400
Crystallite Size (Å)
4
8
12
16
Mn concentration (at%)

Fig.2

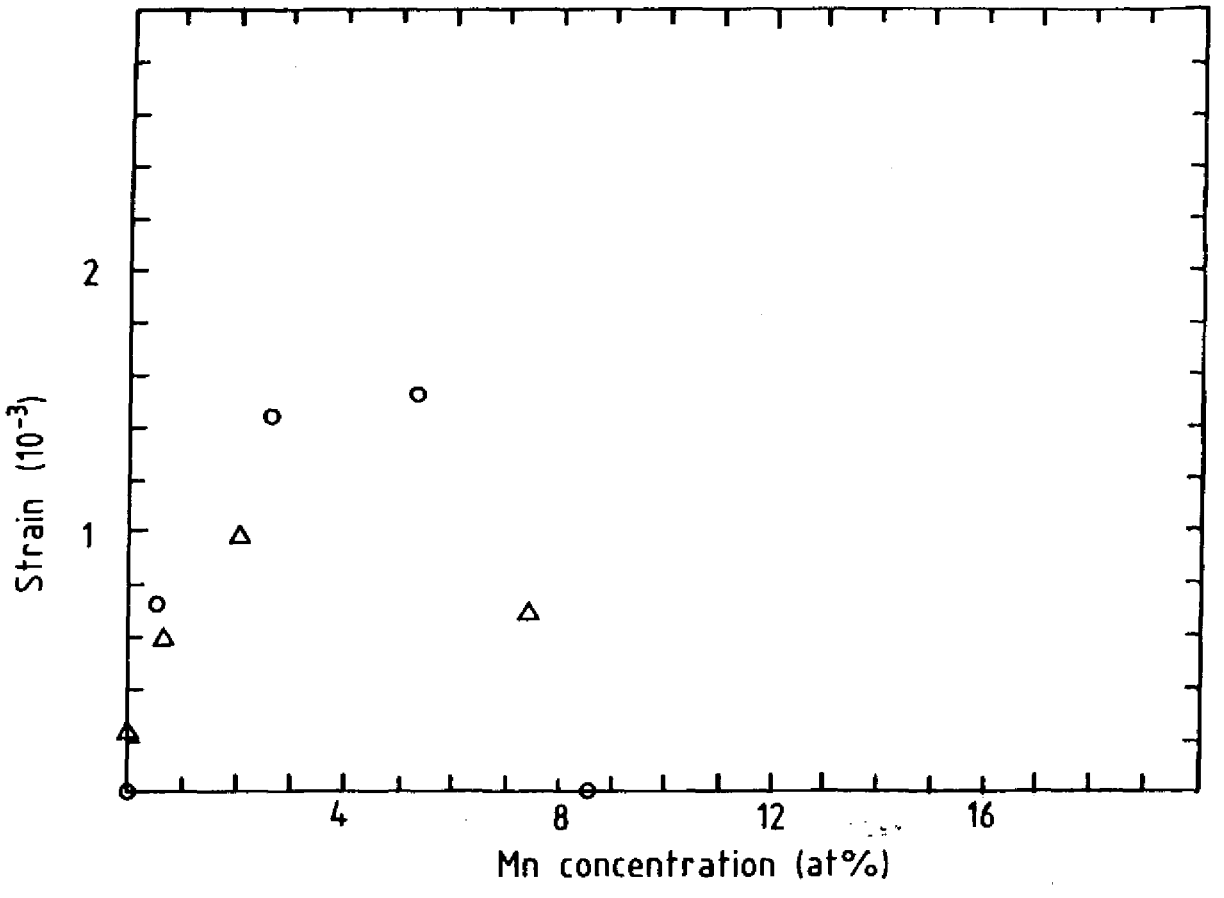
2
1
Strain (10^{-3})
4
8
12
16
Mn concentration (at%)

Fig.3

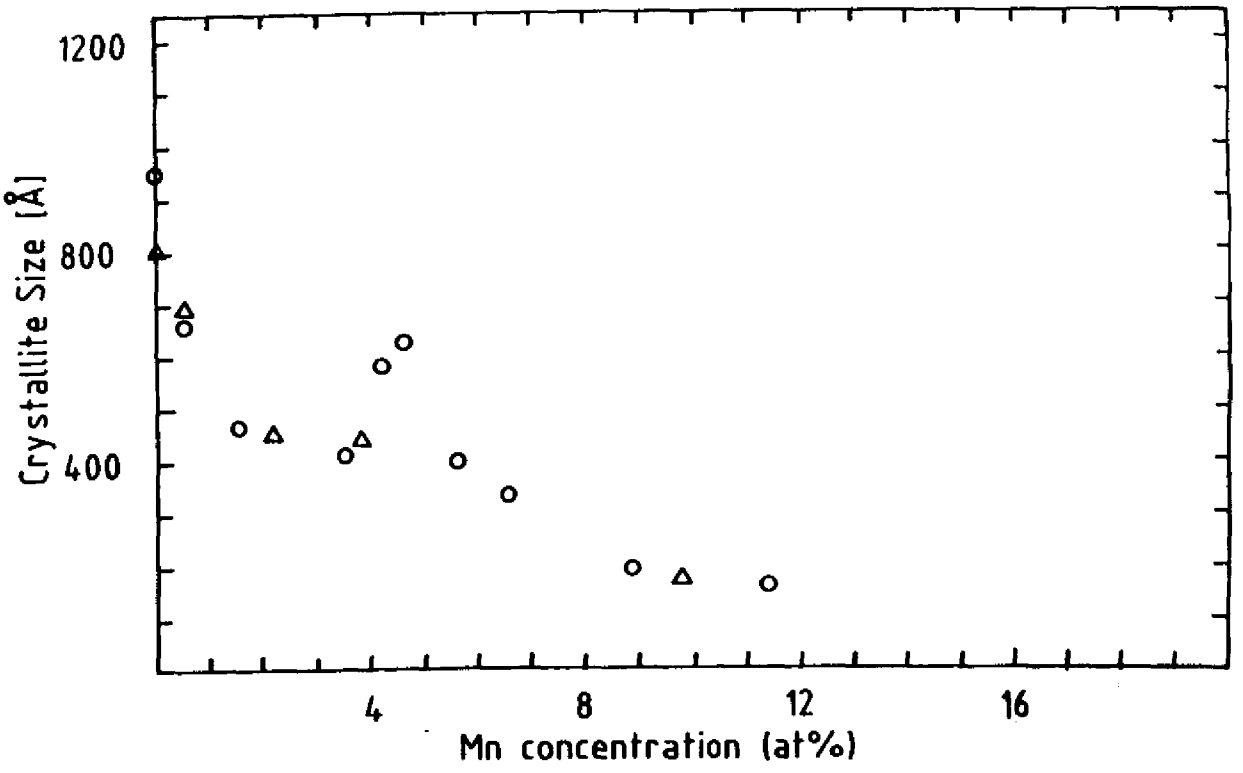
1200
800
400
Crystallite Size (Å)
4
8
12
16
Mn concentration (at%)

Fig.4

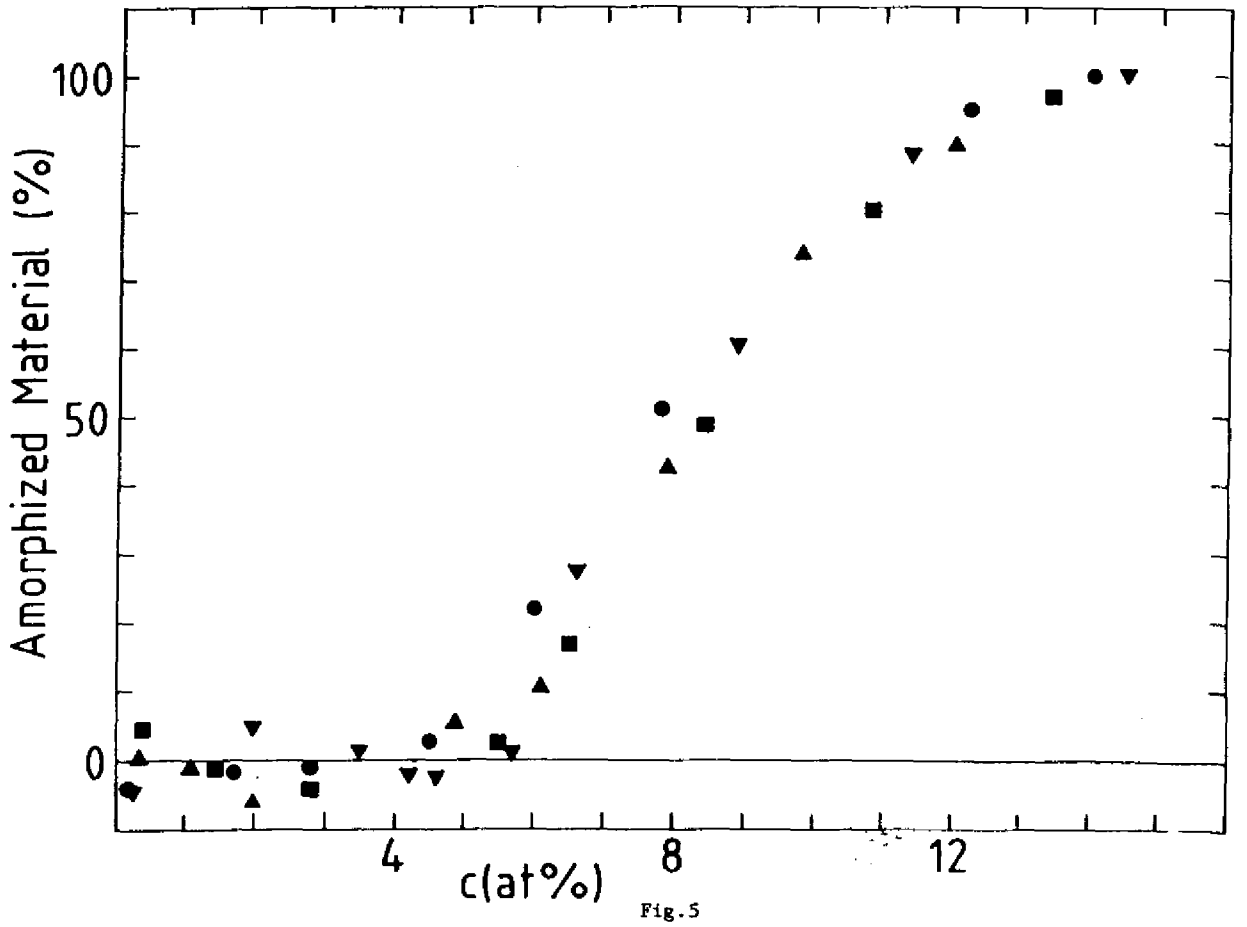
100
50
0
Amorphized Material (%)
4
8
12
c(at%)

Fig.5

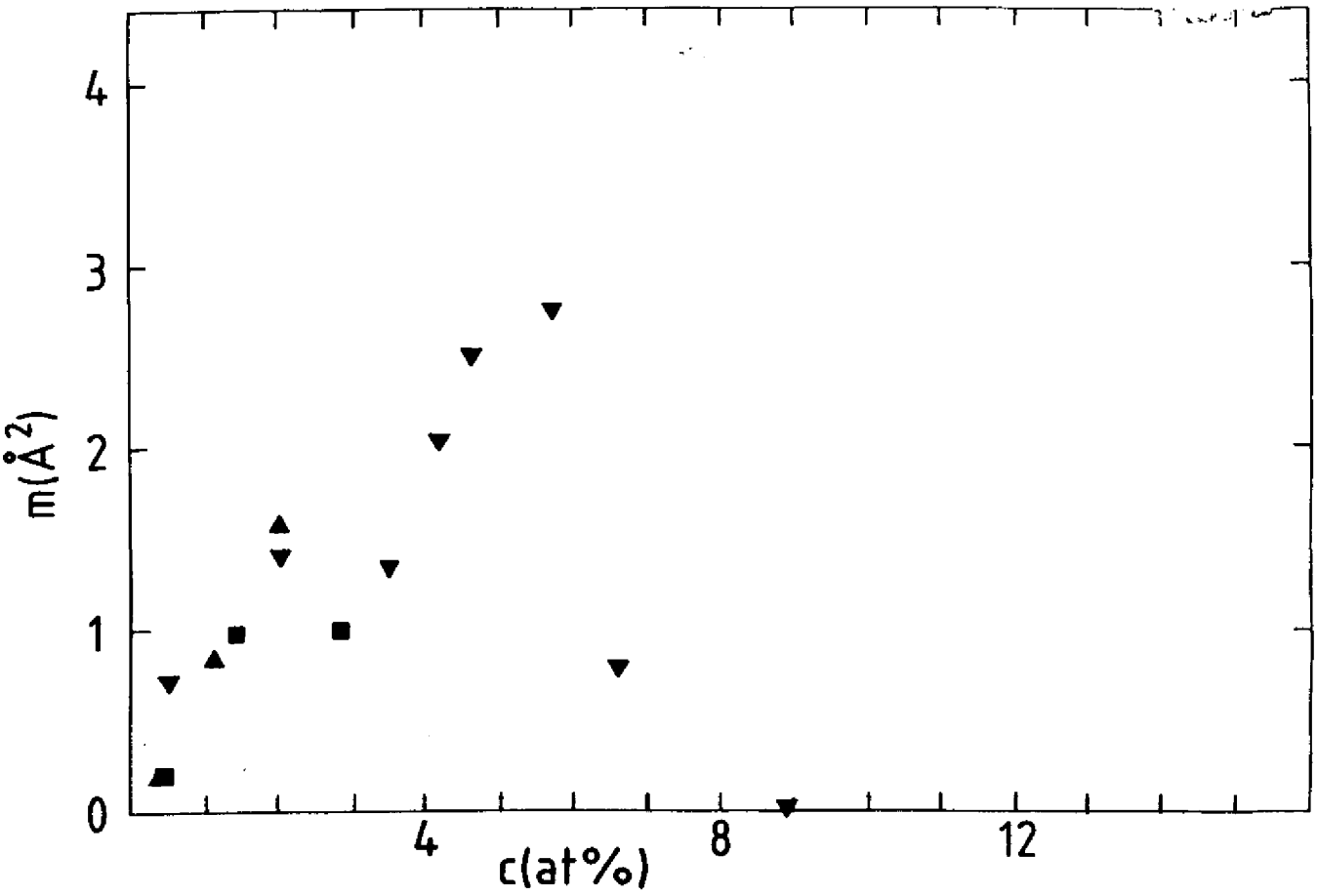

Fig.6

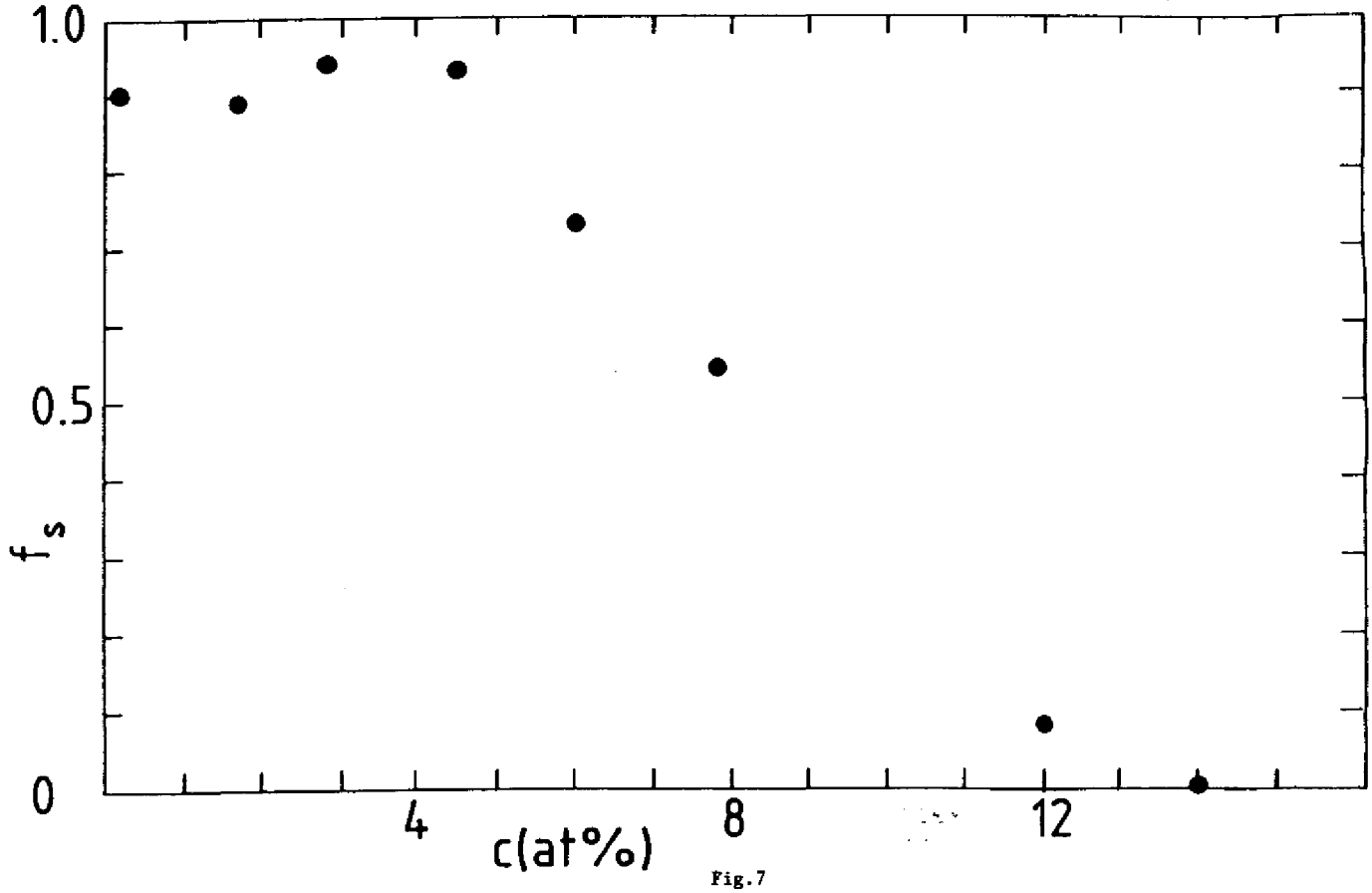

Fig.7

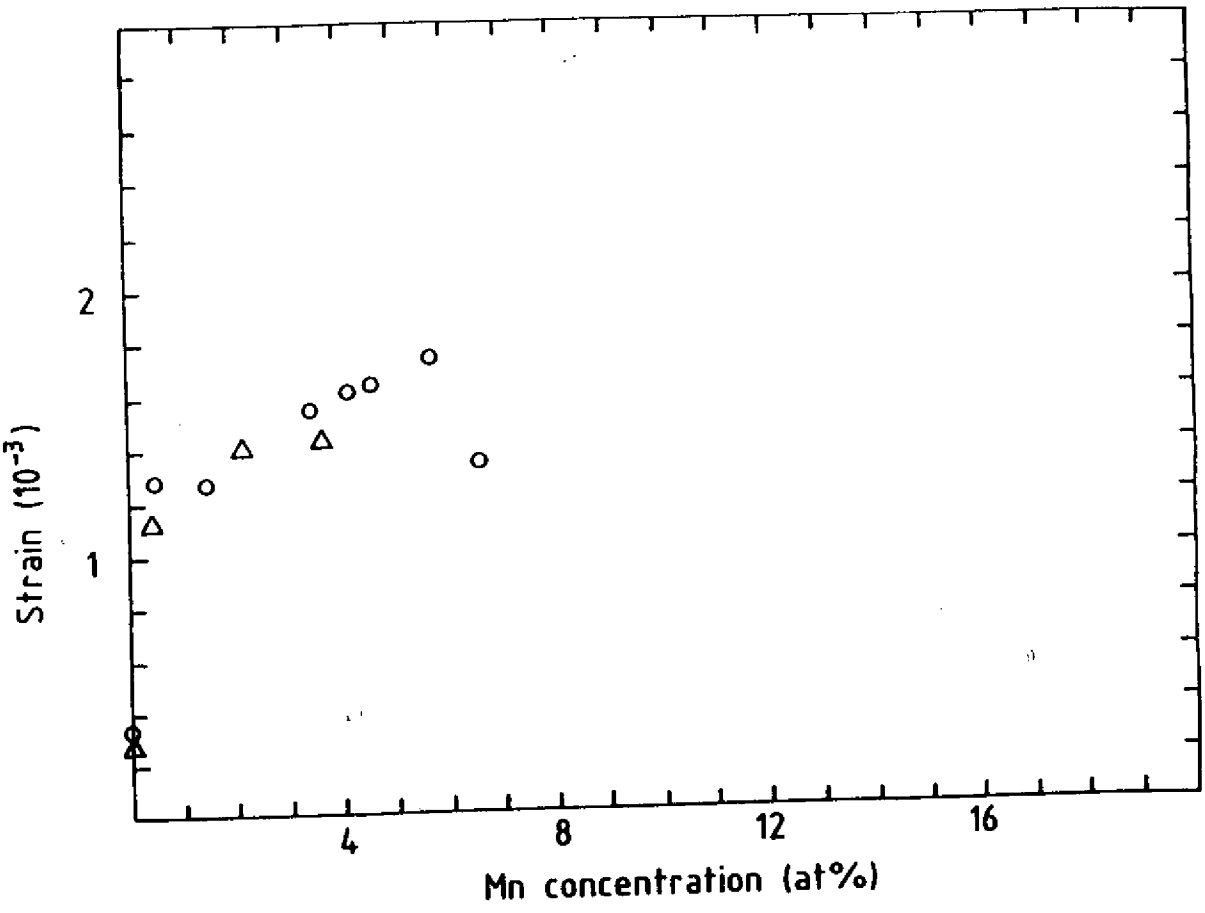

Fig.8